

Orbital Masses: the Usefulness of Diffusion-Weighted Imaging in Lesion Categorization

Z. Fatima · T. Ichikawa · K. Ishigame · U. Motosugi ·
A. B. Waqar · M. Hori · H. Iijima · T. Araki

Received: 9 November 2012 / Accepted: 21 June 2013 / Published online: 12 July 2013
© Springer-Verlag Berlin Heidelberg 2013

Abstract

Introduction Diffusion-weighted imaging (DWI) produces contrast among different kinds of tissues according to their diffusibility characteristics. The purpose of our study was to evaluate the role of DWI including measurement of apparent diffusion coefficient (ADC) values in recognizing benignancy or malignancy of orbital masses.

Methods A total of 39 orbital masses were evaluated visually for signal characteristics on DWI and ADC maps. ADC values were calculated for each lesion. Visual signal characteristics were compared using the Fisher exact test. Receiver operating characteristic (ROC) analysis was carried out to determine sensitivity and specificity for distinguishing malignant from benign lesions using ADC values. The Mann–Whitney U test was applied to compare the ADC values between orbital lymphomas and idiopathic orbital inflammatory (IOI) lesions, and between optic nerve sheath meningiomas and gliomas.

Results Visual assessment revealed no significant difference between benign and malignant lesions on DWI (p -value=0.66). However, visual assessment of ADC maps revealed a statistically significant (p -value \leq 0.0001) between benign and malignant lesions. ROC analysis showed a sensitivity of 83.33% and a specificity of 85.71% when using an optimal cut off ADC value of 0.84×10^{-3} mm²/s for differentiating malignant from benign lesions. Significant differences in mean ADC values were observed between lymphomas and IOI lesions (p -value=0.05), and between optic nerve sheath meningiomas and gliomas (p -value=0.03).

Conclusion DWI is useful for differentiating malignant and benign orbital tumors if accompanied by visual assessment of ADC maps and ADC value calculations.

Keywords Diffusion-weighted imaging · Orbital masses · ADC values

T. Ichikawa, MD, PhD (✉) · Z. Fatima, MBBS, MS ·
K. Ishigame, MD, PhD · U. Motosugi, MD, PhD · T. Araki, MD, PhD
Department of Radiology, University of Yamanashi,
1110 Shimokato, Chuo-shi, Yamanashi 409-3898, Japan
e-mail: ichikawa@yamanashi.ac.jp

A. B. Waqar, MD, PhD
Department of Molecular Pathology, Interdisciplinary Graduate
School of Medicine and Engineering, University of Yamanashi,
1110 Shimokato, Chuo-shi, Yamanashi 409-3898, Japan

M. Hori, MD, PhD
Department of Radiology, School of Medicine, Juntendo
University, 2-1-1 Hongo, Bunkyo-ku, Tokyo 113-8421, Japan

H. Iijima, MD, PhD
Department of Ophthalmology, University of Yamanashi,
1110 Shimokato, Chuo-shi, Yamanashi 409-3898, Japan

Introduction

Magnetic resonance imaging (MRI) is a vital imaging technique for assessing space-occupying lesions of the brain [1]. Although MRI has been used worldwide to detect intra-orbital lesions for many years [2], few recently published studies have addressed its utility for the proper evaluation and characterization of orbital pathologies including masses [3–7]. Diffusion-weighted imaging (DWI) is a specific MR sequence that uses the diffusion of moving water protons to generate a contrast among different kinds of tissues and thus can be a source of valuable information in the assessment of pathological tissues [7, 8].

The orbit is affected by a variety of benign and malignant lesions. Some lesions are diagnosed easily on the basis of

imaging findings such as enhancement characteristics, but sometimes their characterization is difficult and any additional information that can assist the diagnosis greatly facilitates clinical management planning [4, 5].

Many earlier studies suggested that apparent diffusion coefficient (ADC) measurements can help reveal benignancy or malignancy of tumors in the brain, head, and neck, including the orbits [5, 8, 9]; the viable parts within a tumor [10]; and the tumor grade in other organs, such as the liver [11].

The purpose of this study was to evaluate the role of DWI including measurement of ADC values in recognizing benignancy or malignancy of orbital masses.

Methods

Sampling and Selection Criteria

The Institutional Review Board for ethical issues approved this retrospective study. The institutional data base system was searched for patients who had undergone MRI examination for orbital masses from April 2002 to December 2011. A total of 35 patients with 39 lesions (age range, 3–82 years; mean age, 53 years; male to female ratio, 23:12) were selected, excluding those with compromised DWI quality or uncertain clinical diagnosis. All cases of lymphoma ($n=9$ with 10 lesions), metastasis ($n=4$), carcinoma ($n=2$), pleomorphic adenoma ($n=3$), Schwannoma ($n=1$), cavernous hemangioma ($n=2$), and solitary fibrous tumor ($n=1$) were histopathologically proven. Cases of leukemic ($n=1$) (chloroma) and sarcoidotic involvement of the orbit ($n=1$), each with bilateral orbital involvement, were diagnosed clinically on the basis of concomitant systemic illness. These lesions subsequently showed improvement with treatment in follow-up studies. Idiopathic orbital inflammatory (IOI) lesions, also known as pseudoinflammatory tumors ($n=4$ with five lesions), were also diagnosed on clinical grounds, with subsequent resolution by steroid therapy in three out of four cases. The remaining case is in the phase of treatment and follow-up. Clinically suspected cases of meningioma ($n=4$) and glioma ($n=3$) of the optic nerve sheath had other characteristic imaging findings on other MRI sequences, such as a tram-track sign in cases of meningioma [12] and typical fusiform appearance and a downward kink in the mid orbit in two patients of optic nerve sheath glioma associated with neurofibromatosis [13, 14]. A globular appearance was observed in one glioma patient who did not have any other associated condition. Table 1 shows patients' demographics.

MRI Acquisition

All patients were imaged before undergoing biopsy (if performed) on a 1.5 T (GE Healthcare, Milwaukee, WI)

Table 1 Table shows number of each type of lesion with patients' demographics

	No. of lesions (patients)	Mean age (years)	Gender (M:F)	Laterality (right:left)
<i>Malignant</i>				
Lymphoma	10 (9)	68.2	7:2	5:5
Metastasis	4 (4)	61	2:2	2:2
Carcinoma	2 (2)	75	2:0	1:1
Leukemia	2 (1)	53	1:0	1:1
<i>Benign</i>				
Idiopathic orbital inflammatory lesions	5 (4)	45	2:2	3:2
Pleomorphic adenoma	3 (3)	58.6	2:1	2:1
Optic nerve sheath meningioma	4 (4)	60.2	2:2	1:3
Optic nerve sheath glioma	3 (3)	7.3	3:0	0:3
Miscellaneous benign lesions	6 (5)	40.2	2:3	2:4

M male, *F* female

scanner. The routine protocol for imaging the orbits in our department [pre- and postcontrast T1-weighted axial and coronal imaging, and axial and coronal T2-weighted imaging (T2WI) of orbits with fat saturation] and single-shot echo-planar diffusion-weighted imaging sequence was followed. Imaging parameters of DWI were as follows: repetition time (TR)/echo time (TE)=8,000/68 ms; time interval between leading edges of diffusion gradients (Δ)/pulse gradient duration (δ)=39/32 ms; slice thickness/gap, 5 mm/1.5 mm; matrix 128 × 128; field of view (FOV), 24 × 24 cm; number of excitations (NEX)=1; and motion probing gradient pulses along three orthogonal axes using b values of 0 and 1,000 s/mm².

Post-Processing

DWI data were transferred to a Synapse 3D workstation (Fujifilm Medical Systems, USA, Inc.) and ADC maps were generated.

Image Analysis

The signal characteristics on DWI and ADC maps were described as hyperintense for bright or similar signal intensity lesions and as hypointense for those with low signal intensity relative to the normal cortical gray matter.

To calculate the ADC values, the sizes of the regions of interest were adjusted according to the lesion size. Two or more regions of interest were placed in larger lesions and their mean value was used to increase the reliability of the

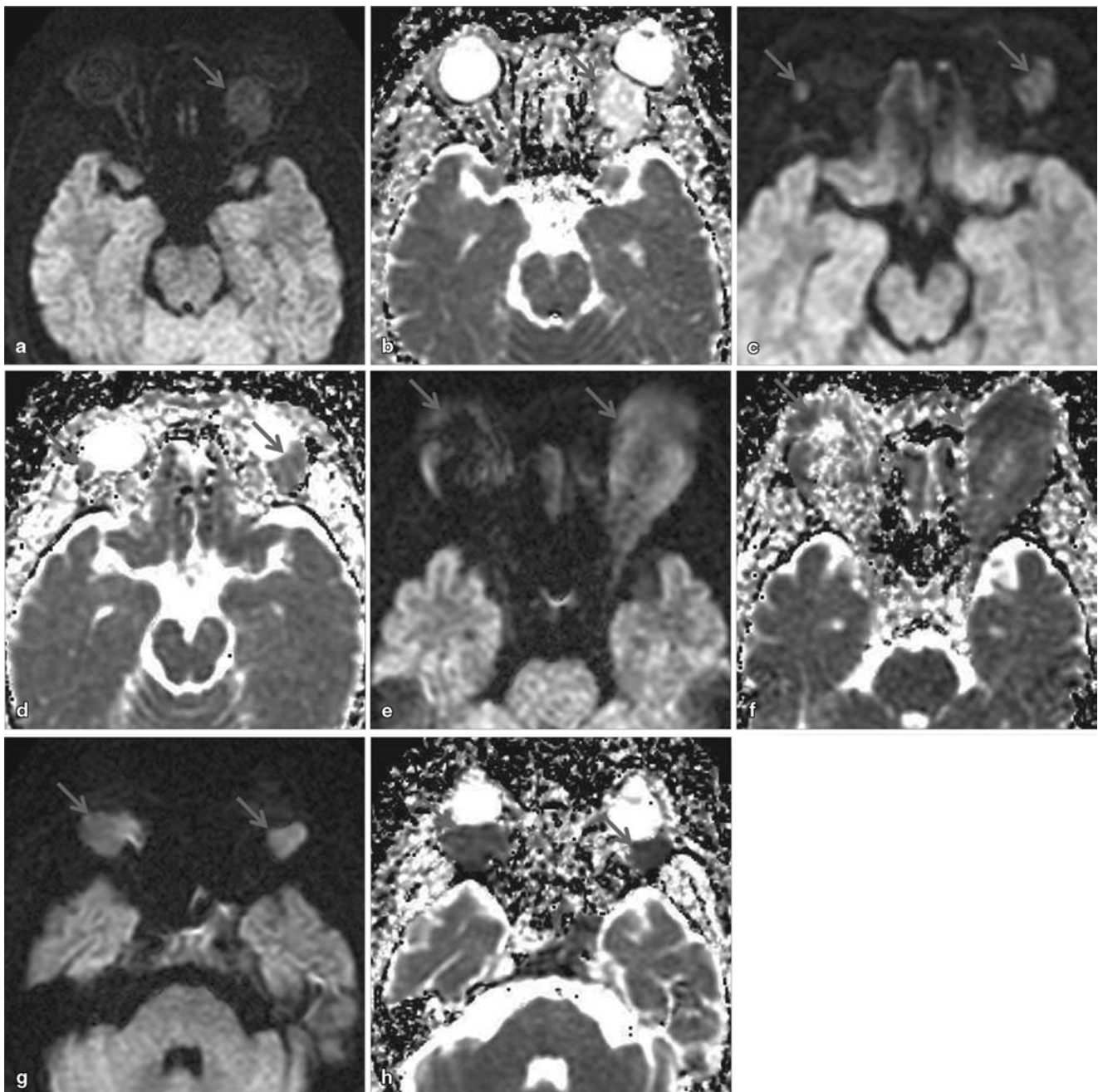


Fig. 1 The diffusion-weighted imaging (DWI) and apparent diffusion coefficient (ADC) maps of benign lesions in **a–d** and of malignant lesions in **e–h**. An intraorbital Schwannoma shows hypointensity on DWI (**a**) and marked hyperintensity on the ADC map (**b**). Bilateral IOI

lesions display moderate hyperintensity on both DWI (**c**) and ADC map (**d**). DW images and ADC maps of bilateral lymphomas (**e, f**) and leukemia (**g, h**); both demonstrate hyperintensity on DWI and marked hypointensity on ADC maps

calculation. Care was taken to avoid the edges of the lesions to exclude the effect of partial volume averaging.

Statistical Analysis

The Fisher exact test was performed to compare the signal characteristics of DWI images and ADC maps between benign and malignant lesions. Receiver operating charac-

teristic (ROC) analysis was carried out to determine the optimal cut-off ADC values, sensitivity, and specificity to differentiate between the malignant and benign lesions. The Mann–Whitney U test was applied to compare the ADC measurements between orbital lymphomas and IOI lesions and between optic nerve sheath meningiomas and gliomas. A two-sided *p*-value of 0.05 was considered significant.

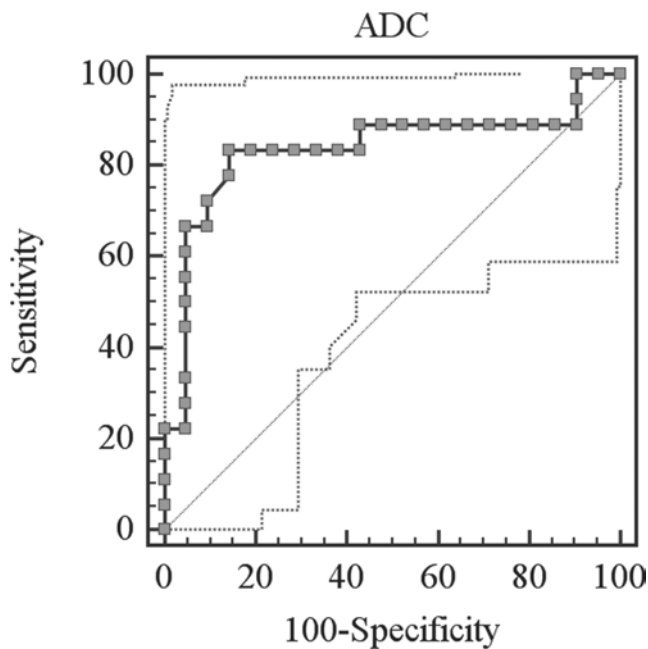


Fig. 2 Receiver operating characteristics curve for differentiating benign and malignant lesions using ADC values. A sensitivity of 83.33%, a specificity of 85.71%, and an optimal cut-off ADC value of $0.84 \times 10^{-3} \text{ mm}^2/\text{s}$ were obtained

Results

Visual assessment of DWI images did not reveal a significant difference (hyperintensity:hypointensity, 17:4 in benign lesions and 16:2 in malignant lesions; p -value=0.66) between benign and malignant lesions. However, the signal characteristics for ADC maps (hyperintensity:hypointensity, 17:4 in benign lesions and 3:15 in malignant lesions; p -value \leq 0.0001) were significantly different in benign vs. malignant lesions (Fig. 1). The mean (SD) ADC values for malignant and benign orbital masses were $0.77 (0.38) \times 10^{-3}$ and $1.23 (0.42) \times 10^{-3} \text{ mm}^2/\text{s}$, respectively. ROC curve analysis showed an optimal cut-off ADC value of $0.84 \times 10^{-3} \text{ mm}^2/\text{s}$, which yielded a sensitivity of 83.33% and a specificity of 85.71% for differentiating malignant from benign lesions (Fig. 2 and Table 2).

The Mann–Whitney U test showed a significant difference in mean (SD) ADC values between lymphomas [$0.61 (0.12) \times 10^{-3} \text{ mm}^2/\text{s}$, $p=0.05$] and IOI lesions [$0.93 (0.35) \times 10^{-3} \text{ mm}^2/\text{s}$] and between optic nerve sheath meningioma [$0.90 (0.08) \times 10^{-3} \text{ mm}^2/\text{s}$] and glioma [$1.31 (0.09) \times 10^{-3} \text{ mm}^2/\text{s}$, $p=0.03$] (Figs. 1c–f, 3, 4a, b, and Table 3).

Table 2 Radiological characteristics, including apparent diffusion coefficient (ADC) values, of patients with benign and malignant orbital masses

	Benign	Malignant	p -value
No. of lesions (patients)	21 (19)	18 (16)	
<i>Signal intensity on DWI</i>			
Hyperintense	17/21 (81%)	16/18 (88.9%)	0.66
Hypointense	4/21 (19%)	2/18 (11.1%)	
<i>Signal intensity on ADC map</i>			
Hyperintense	17/21 (81%)	3/18 (16.6%)	<0.0001
Hypointense	4/21 (19%)	15/18 (83.3%)	
ADC, Mean(SD) ($10^{-3} \text{ mm}^2/\text{s}$)	1.23 (0.42)	0.77(0.38)	<0.0001

DWI diffusion-weighted imaging, *SD* standard deviation

Discussion

Our study confirmed previous results showing that malignant lesions have significantly lower ADC values than benign lesions [5, 7, 15]. The reason for this behavior is thought to be because of the peculiar enlarged and deformed nuclei and hypercellularity characteristics of malignant lesions, thus reducing the available diffusion space for water protons in both the extracellular and intracellular spaces. Malignant lymphomas also show higher cellularity; thus, they are expected to show lower ADC values for the same reason [8].

However, one lesion each of carcinoma and metastasis included in our study showed noticeably high ADC values and hypointensity on DW images. These lesions showed no evidence of cystic changes or areas of necrosis on T2WI. A considerable overlap in ADC values among malignant and benign lesions has been found in many previous studies [1, 5, 8, 9]. The small necrotic foci in the malignant tumors, which are not identifiable at MRI, are presumably the major reason for the high ADCs of these lesions.

Sepahdari et al. [5] found a cut-off ADC value of $1 \times 10^{-3} \text{ mm}^2/\text{s}$, which is slightly larger than that found in our study. Although the malignant lesions in their study included a large proportion of lymphoma lesions (6/16, 37.5%), we had an even greater proportion of lymphoma lesions in our study (10/18, 55.5%). Lymphomatous lesions decrease the mean ADC values of malignant lesions because they tend to have lower ADC values. In short, the relative proportion of different types of malignant as well as benign lesions might affect the mean and cut-off ADC values, therefore producing variable results in different studies.

The reason that visual assessment of benign and malignant lesions did not reveal significant differences on DW images might be explained by the so-called T2 shine-through effect. The signal intensity on DWI can be affected by both the diffusivity of the tissue and the T2 relaxation

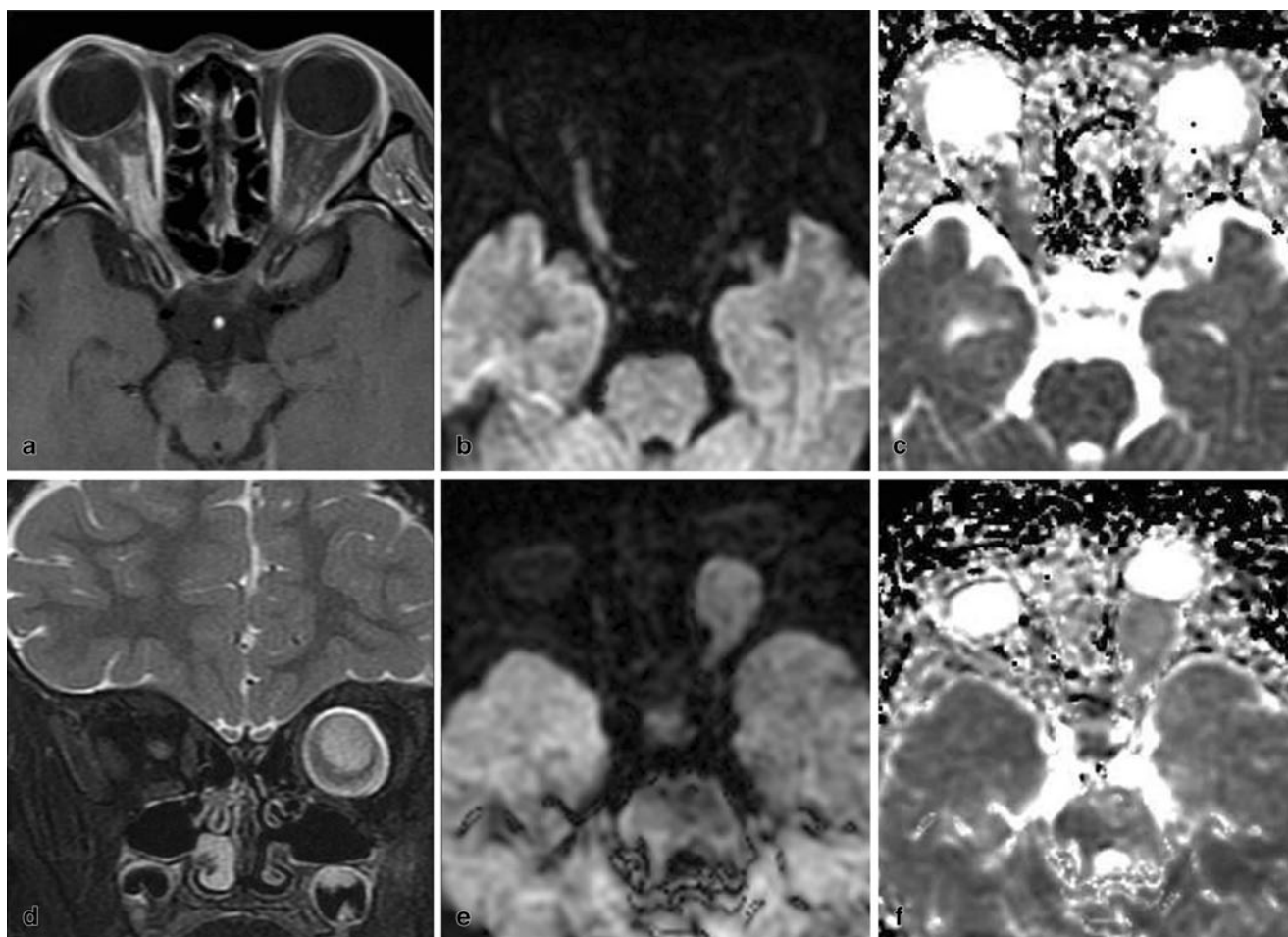


Fig. 3 A right-sided optic nerve sheath meningioma shows a tram-track sign on contrast-enhanced T1-weighted imaging (a), hyperintensity on diffusion-weighted imaging (DWI) (b), and hypointensity on the apparent diffusion coefficient (ADC) map (c). An optic nerve sheath glioma exhibits

globular enlargement on a T2-weighted coronal image (d) and hyperintensity on DWI (e) but a relatively brighter lesion on the ADC map and higher mean ADC values compared with meningioma (f)

time, whereas ADC maps are only affected by diffusibility changes [16]. Rana et al. [17] reported that ADC maps and values tended to be more meaningful than DWI for depicting subtle changes in the content of pus in a case of brain abscess.

Optic nerve gliomas are low-grade tumors, resembling histologically to pilocytic astrocytomas [18], which are reported to have higher ADC values [19]. However, meningiomas are variable in cellularity [5] and hence in ADC values. So the differentiation on the basis of ADC might not be so simple in all cases, although we found a significant difference in ADC values between these two in this study.

The limitations of our study include the small sample size for various types of lesions with some possible effects on the outcome of our study. DWI was performed with relatively thicker (5 mm) slices to improve signal to noise ratio but compromising the spatial resolution, resulting in partial volume effects. This might also be considered as a limiting

factor. The absence of histopathological evidence for some of the benign lesions and the retrospective study design are other limitations of our study.

Conclusion

DWI can be useful for differentiating between malignant and benign orbital tumors if accompanied by visual assessment of ADC maps and ADC value calculations.

Conflict of Interest There are no conflicts of interest to declare.

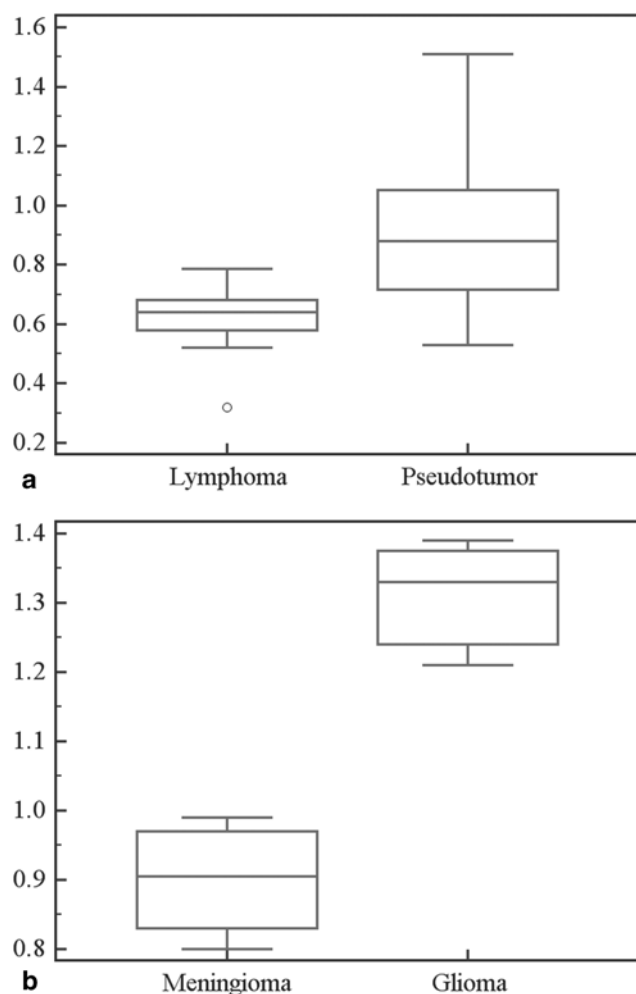


Fig. 4 Box and whisker graphs showing comparison of apparent diffusion coefficient-values between lymphomas and idiopathic orbital inflammatory lesions (pseudotumor) (a) and meningiomas and gliomas (b). Boxes have lines at lower, median, and upper quartile values. Whiskers show extent of remaining data

Table 3 Table shows apparent diffusion coefficient, mean (SD) (10^{-3} mm²/s) of lymphomas vs. idiopathic orbital inflammatory lesions and optic nerve sheath meningiomas vs. gliomas compared by Mann–Whitney U test

Lymphoma	Idiopathic orbital inflammatory lesions	p-value
0.61 (0.12)	0.93 (0.35)	0.05
Optic nerve sheath meningioma	Optic nerve sheath glioma	p-value
0.9 (0.08)	1.31 (0.09)	0.03

References

- Bulakbasi N, Kocaoglu M, Ors F, Tayfun C, Ucoz T. Combination of single-voxel proton MR spectroscopy and apparent diffusion coefficient calculation in the evaluation of common brain tumors. *AJNR Am J Neuroradiol.* 2003;24:225–33.
- Edwards JH, Hyman RA, Vacirca SJ, Boxer MA, Packer S, Kaufman IH, et al. 6 T magnetic resonance imaging of the orbit. *AJR.* 1985;144:1015–20.
- Fatima Z, Motosugi U, Muhi A, Hori M, Ishigame K, Araki T. Diffusion-weighted imaging in optic neuritis. *Can Assoc Radiol J.* 2013;64:51–5.
- Xian J, Zhang Z, Wang Z, Li J, Yang B, Man F, et al. Value of MR imaging in the differentiation of benign and malignant orbital tumors in adults. *Eur Radiol.* 2010;20:1692–702.
- Sepahdari AR, Aakalu VK, Setabutr P, Shiehorteza M, Naheedy JH, Mafee MF. Indeterminate orbital masses: restricted diffusion at MR imaging with echo-planar diffusion-weighted imaging predicts malignancy. *Radiology.* 2010;256:554–64.
- Lope LA, Hutcheson KA, Khademian ZP. Magnetic resonance imaging in the analysis of pediatric orbital tumors: utility of diffusion-weighted imaging. *J AAPOS.* 2010;14:257–262.
- Politi LS, Forghani R, Godi C, Resti AG, Ponzoni M, Bianchi S, et al. Ocular adnexal lymphoma: diffusion-weighted MR imaging for differential diagnosis and therapeutic monitoring. *Radiology.* 2010;256:565–74.
- Wang J, Takashima S, Takayama F, Kawakami S, Saito A, Matsushita T, et al. Head and neck lesions: characterization with diffusion-weighted echo-planar MR imaging. *Radiology.* 2001;220:621–30.
- Eida S, Sumi M, Sakihama N, Takahashi H, Nakamura T. Apparent diffusion coefficient mapping of salivary gland tumors: prediction of the benignancy and malignancy. *AJNR Am J Neuroradiol.* 2007;28:116–21.
- Razek AA, Megahed AS, Denewar A, Motamed A, Tawfik A, Nada N. Role of diffusion-weighted magnetic resonance imaging in differentiation between the viable and necrotic parts of head and neck tumors. *Acta Radiol.* 2008;49:364–70.
- Muhi A, Ichikawa T, Motosugi U, Sano K, Matsuda M, Kitamura T, et al. High-b-value diffusion-weighted MR imaging of hepatocellular lesions: estimation of grade of malignancy of hepatocellular carcinoma. *J Magn Reson Imaging.* 2009;30:1005–11.
- Kanamalla US. The optic nerve tram-track sign. *Radiology.* 2003;227:718–9.
- Shapey J, Danesh-Mayer HV, Kaye AH. Diagnosis and management of optic nerve glioma. *J Clin Neurosci.* 2011;18:1585–91.
- Miller NR. Primary tumors of the optic nerve and its sheath. *Eye.* 2004;18:1026–37.
- Razek AA, Elkhamary S, Mousa A. Differentiation between benign and malignant orbital tumors at 3-T diffusion MR-imaging. *Neuroradiology.* 2011;53:517–22.
- Schaefer PW, Gonzalez RG, Hunter G, Wang B, Koroshetz WJ, Schwamm LH. Diagnostic value of apparent diffusion coefficient hyperintensity in selected patients with acute neurologic deficits. *J Neuroimaging.* 2001;11:369–80.
- Rana S, Albayram S, Lin DDM, Yousem DM. Diffusion-weighted imaging and apparent diffusion coefficient maps in a case of intracerebral abscess with ventricular extension. *AJNR Am J Neuroradiol.* 2002;23:109–12.
- Jost SC, Ackerman JW, Garbow JR, Manwaring LP, Gutmann DH, McKinstry RC. Diffusion-weighted and dynamic contrast-enhanced imaging as markers of clinical behavior in children with optic pathway glioma. *Pediatr Radiol.* 2008;38:1293–9.
- Pavlis G, Pavlis G, Rados M. Diffusion differences between pilocytic astrocytomas and grade II ependymomas. *Radiol Oncol.* 2011;45:97–101.